A terahertz plastic wire based evanescent field sensor for high sensitivity liquid detection

Borwen You[1], Tze-An Liu[2], Jin-Long Peng[2], Ci-Ling Pan[3] and Ja-Yu Lu[1*]

[1] *Institute of Electro-Optical Science and Engineering and Advanced Optoelectronic Technology Center, National Cheng Kung University, 1 University Road, Tainan 70101, Taiwan, R.O.C.*

[2] *Center for Measurement Standards, Industrial Technology Research Institute, 321, Section 2, Kuang Fu Road, Hsinchu 30011, Taiwan, R.O.C.*

[3] *Department of Photonics and Institute of Electro-Optical Engineering, National Chiao Tung University, 1001 University Road, Hsinchu 30010, Taiwan, R.O.C.*

**jayu@mail.ncku.edu.tw*

Abstract: A highly sensitive detection method based on the evanescent wave of a terahertz subwavelength plastic wire was demonstrated for liquid sensing. Terahertz power spreading outside the wire core makes the waveguide dispersion sensitive to the cladding index variation, resulting in a considerable deviation of waveguide dispersion. Two liquids with transparent appearances, water and alcohol, are easily distinguished based on the waveguide dispersion, which is consistent with theoretical predictions. A melamine alcohol solution with various concentrations is identified successfully, and the detection limit is up to 20ppm, i.e. equivalent to the index variation on the order of 0.01.

©2009 Optical Society of America

OCIS codes: (060.2370) Fiber optics sensors; (130.6010) Sensors; (230.7370) Waveguides; (300.6495) Spectroscopy, terahertz.

References and links

1. L. Cheng, H. Shin'ichiro, A. Dobroiu, C. Otani, K. Kawase, T. Miyazawa, and Y. Ogawa, "Terahertz-wave absorption in liquids measured using the evanescent field of a silicon waveguide," Appl. Phys. Lett. **92**(18), 181104 (2008).
2. M. Walther, M. R. Freeman, and F. A. Hegmann, "Metal-wire terahertz time-domain spectroscopy," Appl. Phys. Lett. **87**(26), 261107 (2005).
3. Y. Sun, X. Xia, H. Feng, H. Yang, C. Gu, and L. Wang, "Modulated terahertz responses of split ring resonators by nanometer thick liquid layers," Appl. Phys. Lett. **92**(22), 221101 (2008).
4. A. Ibraheem, I. Al-Naib, C. Jansen, and M. Koch, "Thin-film sensing with planar asymmetric metamaterial resonators," Appl. Phys. Lett. **93**, 083507 (2008).
5. J. F. O'Hara, R. Singh, I. Brener, E. Smirnova, J. Han, A. J. Taylor, and W. Zhang, "Thin-film sensing with planar terahertz metamaterials: sensitivity and limitations," Opt. Express **16**(3), 1786–1795 (2008).
6. H. Kur, "Coupled-resonator optical waveguides for biochemical sensing of nanoliter volumes of analyte in the terahertz region," Appl. Phys. Lett. **87**(24), 241119 (2005).
7. F. Miyamaru, S. Hayashi, C. Otani, K. Kawase, Y. Ogawa, H. Yoshida, and E. Kato, "Terahertz surface-wave resonant sensor with a metal hole array," Opt. Lett. **31**(8), 1118–1120 (2006).
8. H. Yoshida, Y. Ogawa, Y. Kawai, S. Hayashi, A. Hayashi, C. Otani, E. Kato, F. Miyamaru, and K. Kawase, "Terahertz sensing method for protein detection using a thin metallic mesh," Appl. Phys. Lett. **91**(25), 253901 (2007).
9. S. Yoshida, E. Kato, K. Suizu, Y. Nakagomi, Y. Ogawa, and K. Kawase, "Terahertz sensing of thin poly(ethylene terephthalate) film thickness using a metallic mesh," Appl. Phys. Express **2**, 012301 (2009).
10. M. Nagel, P. Haring Bolivar, M. Brucherseifer, H. Kurz, A. Bosserhoff, and R. Bu¨ttner, "Integrated THz technology for label-free genetic diagnostics," Appl. Phys. Lett. **80**(1), 154–156 (2002).
11. A. Chakraborty, and N. Guchhait, "Inclusion complex of charge transfer probe 4-amino-3-methyl benzoic acid methyl ester (AMBME) with b-CD in aqueous and non-aqueous medium: medium dependent stoichiometry of the complex and orientation of probe molecule inside b-CD nanocavity," J. Incl. Phenom. Macrocycl. Chem. **62**(1-2), 91–97 (2008).
12. N. A. Mortensen, S. Xiao, and J. Pedersen, "Liquid-infiltrated photonic crystals: enhanced light-matter interactions for lab-on-a-chip applications," Microfluid Nanofluid **4**(1-2), 117–127 (2008).
13. L.-J. Chen, H.-W. Chen, T.-F. Kao, J.-Y. Lu, and C.-K. Sun, "Low-loss subwavelength plastic fiber for terahertz waveguiding," Opt. Lett. **31**(3), 308–310 (2006).

#117682 - $15.00 USD Received 24 Sep 2009; revised 23 Oct 2009; accepted 23 Oct 2009; published 27 Oct 2009

14. A. Dupuis, J.-F. Allard, D. Morris, K. Stoeffler, C. Dubois, and M. Skorobogatiy, "Fabrication and THz loss measurements of porous subwavelength fibers using a directional coupler method," Opt. Express **17**(10), 8012–8028 (2009).
15. J.-Y. Lu, C.-M. Chiu, C.-C. Kuo, C.-H. Lai, H.-C. Chang, Y.-J. Hwang, C.-L. Pan, and C.-K. Sun, "Terahertz scanning imaging with a subwavelength plastic fiber," Appl. Phys. Lett. **92**(8), 084102 (2008).
16. C.-M. Chiu, H.-W. Chen, Y.-R. Huang, Y.-J. Hwang, W.-J. Lee, H.-Y. Huang, and C.-K. Sun, "All-terahertz fiber-scanning near-field microscopy," Opt. Lett. **34**(7), 1084–1086 (2009).
17. L. Tong, J. Lou, and E. Mazur, "Single-mode guiding properties of subwavelength-diameter silica and silicon wire waveguides," Opt. Express **12**(6), 1025–1035 (2004).
18. J. W. Lamb, "Miscellancous data on materials for millimetre and submillimetre optics," Int. J. Infrared. Milli. **17**, 1996–2034 (1996).
19. J. Lou, L. Tong, and Z. Ye, "Modeling of silica nanowires for optical sensing," Opt. Express **13**(6), 2135–2140 (2005).
20. H.-W. Chen, Y.-T. Li, C.-L. Pan, J.-L. Kuo, J.-Y. Lu, L.-J. Chen, and C.-K. Sun, "Investigation on spectral loss characteristics of subwavelength terahertz fibers," Opt. Lett. **32**(9), 1017–1019 (2007).
21. B. Ferguson, and X.-C. Zhang, "Materials for terahertz science and technology," Nat. Mater. **1**(1), 26–33 (2002).
22. H. Kitahara, T. Yagi, K. Mano, and M. W. Takeda, "Dielectric characteristics of water solutions of ethanol in the terahertz region," J. Korean Phys. Soc. **46**, 82–85 (2005).
23. L. Thrane, R. H. Jacobsen, P. Uhd Jepsen, and S. R. Keiding, "THz reflection spectroscopy of liquid water," Chem. Phys. Lett. **240**(4), 330–333 (1995).
24. B. E. A. Saleh, and M. C. Teich, *fundamentals of photonics* (John Wiley & Sons, New York, NY 1991).
25. J. Lou, L. Tong, and Z. Ye, "Dispersion shifts in optical nanowires with thin dielectric coatings," Opt. Express **14**(16), 6993–6998 (2006).
26. C.-L. Chen, *elements of optoelectronics and fiber optics*, chap.8 (Times Mirror Higher Education Group, Inc. company, 1996).
27. A. Sano, Kawasaki, T. Kuroishi, Chiba, Y. Miyazaki, Machida, S. Yokoyama, Yokohama, K. Matsuura, "Easily soluble polyethylene powder for the preparation of fibers or films having high strength and high elastic modulus," united states patent 4760120 (1988). *http://www.freepatentsonline.com/4760120.pdf*
28. IARC Monographs on the Evaluation of Carcinogenic Risks to Humans, "Some chemicals that cause tumours of the kidney or urinary bladder in rodents, and some other substances". *http://monographs.iarc.fr/ENG/Monographs/vol73/index.php*
29. R. E. N. Baozeng, L. I. Chen, Y. U. A. N. Xiaoliang, and W. A. N. G. Fu'an, "Determination and correlation of melamine solubility," Chin. J. Chem. Eng. **54**(7), 1001–1003 (2003).

1. Introduction

Minute material detection has received considerable interest in genomic engineering, lab-on-a-chip, and forensic medicine applications. Noninvasive and label-free molecular detection is easily achieved based on terahertz (THz) fingerprint spectra because their absorption bands, originating from molecular transitions between vibrational or rotational energy levels, are located in the THz frequency range. THz technology has been extensively adopted for minute material detection in the recent decade. A related method measures the relative absorption or molecular characteristic absorption spectrum, such as the silicon waveguide [1] and metal wire [2]. However, for increasing the sensitivity, it requires several milligrams of powders or a high concentration solution [1,2]. Another means of detecting a slight amount of materials is based on refractive index sensitive THz devices, such as metamaterials [3–5], coupled-resonator optical waveguide [6] and metal hole arrays [7–9]. By utilizing a thin film micro-strip line (TFMS), Nagel *et al.* [10] detected the deposited DNA with femto-mol level sensitivity based on the THz resonant band shift of TFMS by varying the sample indexes. A chip-based THz device with a high sensitivity is advantageous for integration with various biochips and planer arrays for multiplexing. However, the TFMS is restricted in noninvasive remote sensing due to the limited transmission length. In addition, the solvents of samples deposited on the micro-strip line waveguide should be evaporated in the process of manipulating samples, and the changed surroundings would possibly modify the intrinsic properties of samples [11]. The subwavelength plastic wire delivered the evanescent wave with low THz photon energy and allowed for non-invasive sensing without sample contact; therefore, it could reduce the restriction mention above. In addition to its flexibility for remotely detecting a sample placed anywhere, such a scheme allows easy integration with biochip or microfludic channels for molecular sensing [12].

THz transmission via subwavelength plastic wire has been demonstrated, in which more than 90% of the THz power is guided outside the wire core [13]. Besides decreasing the THz

#117682 - $15.00 USD Received 24 Sep 2009; revised 23 Oct 2009; accepted 23 Oct 2009; published 27 Oct 2009
(C) 2009 OSA

propagation loss incurred by wire absorption, the enhanced evanescent wave increases the overlapped interaction between sample and THz wave, possibly increasing the sensitivity and decreasing required amounts of the sample placed around the plastic wire. THz subwavelength plastic wire is characterized by its easy availability, low loss, low dispersion [14] and efficient coupling by quasi-optics [13], which is highly promising for biomedical imaging [15,16], remote sensing, and biochip applications.

This work demonstrates the feasibility of an evanescent wave sensor based on the subwavelength plastic wire for liquid sensing. The enhanced evanescent wave sensitizes waveguide dispersion of wire to the refractive index of wire cladding. Slightly varying the cladding index can significantly change waveguide dispersion. The dispersion deviation of guided THz wave is evaluated, and two liquids, i.e. water and alcohol, are easily distinguished between each other, which is consistent with theoretical predictions. A melamine alcohol solution with different concentrations is then identified successfully with a detection limit of 20ppm, implying that detection of index variation is on the order of 0.01. The proposed sensing method is highly promising for food quality control, illicit drugs or explosives detection, as well as molecular dynamic characterization in living cell specimens.

2. Evanescent wave of THz subwavelength plastic wire

The THz subwavelength plastic wire used in this experiment has a circular cross-section, an infinite air-cladding, and a step-index profile [13,17]. The wire core is made of polystyrene (PS), in which the refractive index is 1.59 [18]. Due to the thin core and low core index, a large portion of THz power is transmitted in the air cladding [13]. It also means the power distribution profile of the THz pulse propagating on the PS wire is wavelength dependent. For instance, the calculated fractional THz power in the air cladding for a 300μm-core-diameter-PS wire exceeds 70% when the wavelength exceeds 1mm, as illustrated in Fig. 1(a). This finding implies that the long-wavelength portion of the THz pulse extends further into the air than the short-wavelength, as shown in the inset in Fig. 1(a). The long-wavelength portion possesses an enhanced evanescent wave, subsequently reducing the propagation loss [13] and allowing high sensitivity detection of a medium that surrounds the wire core [19]. Using the vector Maxwell's Eqs. (17), the waveguide dispersion of guided THz pulse on a 300μm-core-diameter-PS wire was determined for various cladding indices. Figure 1(b) shows the calculated wavelength-dependent waveguide dispersions of a THz subwavelength wire with various cladding indices, where normalized with respect to the lowest minimum value, i.e. the case of an air cladding, such that the dispersion minimum of the cladding index of 1.00 curve is normalized to −1. The dip of normalized waveguide dispersion (deep point of curve in Fig. 1(b)) becomes less negative and shifts towards a short wavelength when the cladding index increases [17]. The percentage variation of negative waveguide dispersion, defined as ΔD_{WG}, is approximately proportional to the increasing cladding index. For instance, a PS wire is observed to have around 1%- ΔD_{WG} per 0.01-increase in the cladding index. For the subwavelength THz wire sensor, the deviation of dispersion dip is resulted from the evanescent THz wave transmitted along different specimens with various refractive indices. The cladding index is changed owing to a certain volume of air in the cladding being replaced by the higher index test samples. Based on the detection mechanism, the sensitive scheme to detect refractive index is allowed to identify various specimens without broadband THz transmission which is necessary for detecting THz absorption spectrum of materials. And hence the sensing performance would not be restricted by the deliverable bandwidth even though the transmitted bandwidth of THz subwavelength fiber is typically around 200GHz, which is dependent on the wire length and core absorption loss [20]. By implementing this concept into practice, subwavelength THz wire is a promising alternative for the detection of minute index variations.

#117682 - $15.00 USD Received 24 Sep 2009; revised 23 Oct 2009; accepted 23 Oct 2009; published 27 Oct 2009
(C) 2009 OSA

3. Experimental setup and waveguide dispersion measurement

By using the THz time-domain spectroscopy (THz-TDS) [21] system, the experiment attempted to evaluate and characterize the waveguide dispersion of PS wire with various media that surrounded the wire core. The configuration in Fig. 2(a) contains a mode-locked

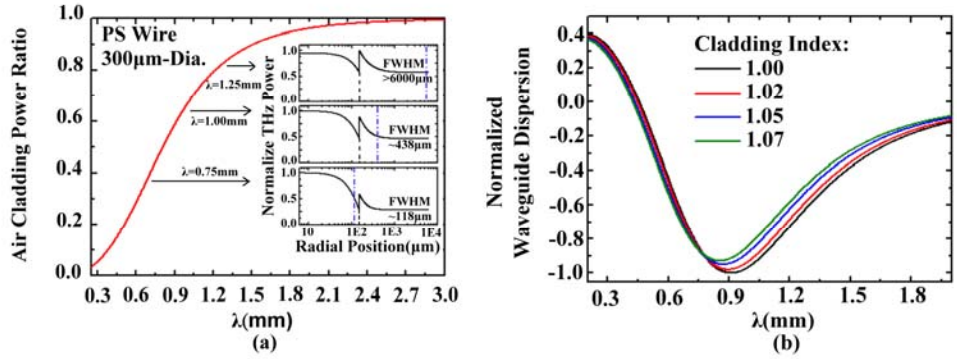

Fig. 1. (a) Fractional power in the air cladding for a 300μm-core-diameter-PS wire. The inset shows the THz power distribution across the PS wire. The black dash line indicates the radius of PS wire (150μm) and the blue dash dot line represents the full with of half maximum (FWHM) range of HE_{11} mode. (b) Normalized waveguide dispersion of 300μm-core-diameter PS wire with various cladding indexes ranging from 1.00 to 1.07.

Ti:sapphire laser with a center wavelength of 800nm, 100fs-pulse duration and 100MHz-repetition rate, a THz emitter, as well as a THz detector. The THz emitter and detector are both low-temperature-GaAs-based photoconductive antennas with a 5μm electrode gap. The generated THz wave was coupled to a 300μm-core-diameter-PS wire by two off-axis parabolic mirrors, collimated by a THz lens, and focused on the THz photoconductive antenna for detection. A 300μm-core-diameter-PS wire with length of 15cm is used for liquid sensing experiment. After THz pulse propagated through a 15cm-long air-clad PS wire, the measured signal/noise ratio (SNR) is around 10^4. The measured attenuation constant of a 300μm-core-diameter-PS wire is illustrated in Fig. 2(b) and the minimum attenuation is as low as 0.01cm^{-1}. A sample holder made of polypropylene (PP) contained a 6mm-wide and 0.5mm-deep channel, which was filled with the test sample. A 10 μm thick polyethylene (PE) film was attached on the top of the PP holder to prevent evaporation of the liquid sample. In the experiment, alcohol and water were used as the liquid samples with distinct THz refractive indices 2.60 and 1.45 [22,23], respectively, at 0.9mm wavelength. Two PP holders with different lengths, i.e. 1mm and 3mm respectively, were used to evaluate the waveguide dispersion in order to acquire the phase difference of THz pulse propagating along the PS wire and through the test samples. The inset in Fig. 2(a) illustrates one portion of the evanescent field interacting with the sample, and the other portion of the field is leaking into the air. Due to the high attenuation of liquid sample, a specimen was placed beneath the PS wire with a separation distance D_1 of around several hundred micrometers to sustain an adequate SNR (>100) of THz wave, while insuring a good overlap between THz evanescent wave and the specimen, as shown in the inset in Fig. 2(a). As the illustration of Fig. 2(b), the attenuation of the THz wave propagated on a 300μm-core-diameter-PS wire across a 3mm-long liquid-filled PP holder is increased from 0.01 to 1cm^{-1} in 0.9~1.1mm-wavelength range with the separation D_1 of 0.43mm. Even though the SNR is decreased from 10^4 to 100, it is sufficient in the work to acquire the phase information for sensing a small amount of liquids.

In the study, the phase difference for THz wave transmitted along the wire with and without liquid samples is described as follows,

$$\Delta\varphi \equiv \left(\varphi_{sL1} - \varphi_{airL1}\right) - \left(\varphi_{sL2} - \varphi_{airL2}\right) \quad (1)$$

#117682 - $15.00 USD Received 24 Sep 2009; revised 23 Oct 2009; accepted 23 Oct 2009; published 27 Oct 2009
(C) 2009 OSA

where φ_{sL1} and φ_{airL1} represent the phases accumulated by the THz pulse that passed through a L_1-long PP holder with and without a sample, respectively. Similarly, φ_{sL2} and φ_{airL2} refer to the phases of THz pulse propagating through L_2-long PP holder with the same depth and width as L_1-long PP holder. Notably, according to Eq. (1), the phase difference considered here is only contributed from the THz wave along the $|L_1 - L_2|$-long PS wire with the sample in the cladding region. The effective index of THz wave propagated on the wire and propagation constant, $\beta = 2\pi n_{eff}/\lambda$, can be derived by substituting $\Delta\varphi$ in Eq. (2).

$$n_{eff} = \frac{\lambda \cdot \Delta\varphi}{2\pi(L_2 - L_1)} + 1 \tag{2}$$

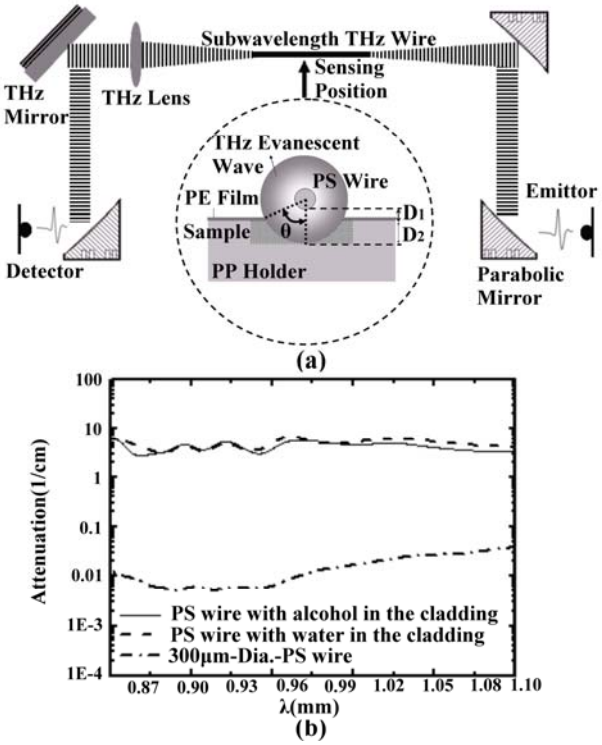

Fig. 2. (a) Experimental setup for THz evanescent wave sensing by using a subwavelength plastic wire. The inset illustrates the cross section of interaction between THz evanescent wave and the sample where D_1 refers to the separation between wire and top surface of sample and D_2 denotes the depth of the PP holder. (b) The attenuation of THz pulse propagated on an air-clad PS wire (thick dash dot line), and on a PS wire across an alcohol-filled (thin solid line) and a water-filled (thick dash line) PP sample holders. The core diameter of PS wire is 300μm.

The measured waveguide dispersion can be straightforwardly calculated from Eqs. (3) and (4) [24] in which V_g represents the THz group velocity along the PS wire with sample cladding. Different samples in the cladding of PS wire influence the propagation features of THz wave, such as the effective index and propagation constant, thus shifting the wavelength-dependent waveguide dispersion curve, as illustrated in Fig. 1(b).

$$V_g = -\frac{2\pi C}{\lambda^2} \cdot \frac{1}{d\beta / d\lambda} \tag{3}$$

#117682 - $15.00 USD Received 24 Sep 2009; revised 23 Oct 2009; accepted 23 Oct 2009; published 27 Oct 2009
(C) 2009 OSA

$$D_{wg} = \frac{d(V_g^{-1})}{d\lambda} \tag{4}$$

4. Sensing results and discussions

The geometrical configuration in the inset in Fig. 2(a) illustrates one portion of THz evanescent field interacting with the samples and the other leaking into the air. For the THz wave on the plastic wire, this resembles a new cladding with an effective index, as attributed to both the air and the sample, which can be defined as follows,

$$n_{Eff,clad} = n_{air} \cdot \sigma + n_{sample} \cdot (1 - \sigma) \tag{5}$$

where σ denotes the fractional power of evanescent THz wave in the air and 1-σ is that in the sample. The index of air, n_{air}, equals 1 and n_{sample} refers to the refractive index of test sample in THz frequency range.

According to Eqs. (6) and (7), the power percentage in the air, σ, could be estimated from the geometric parameters, including the wire radius r, distance D_1, and channel depth D_2 as shown in the inset in Fig. 2(a).

$$\sigma = 1 - \frac{2\theta}{360} \tag{6}$$

$$\theta = \cos^{-1}\left(\frac{r + D_1}{r + D_1 + D_2}\right) \tag{7}$$

In the liquid sensing experiment, the estimated air percentage σ is approximately 68% for D_1 of 0.43mm, channel depth D_2 of 0.5mm, and wire radius r of 0.15mm. The effective cladding index can be calculated based on Eq. (5) from the refractive index of a liquid and the air percentage in the sensing condition. Based on the estimated effective cladding index, the theoretical waveguide dispersion of THz pulse along the PS wire transmitting through a liquid sample can thus be obtained based on Eqs. (3) and (4). In the study, the refractive indices of water and alcohol in THz are considered as 2.60 and 1.45 [22,23], respectively, at 0.9mm wavelength. By incorporating 68%-σ into Eq. (5), the effective cladding indices are therefore 1.144 and 1.512 for alcohol and water, respectively. Figure 3(a) shows the simulated wavelength-dependent waveguide dispersion, indicating a 58% variation of the dip of waveguide dispersion between alcohol and water. Figure 3(b) shows the measured waveguide dispersion of THz pulse propagated on the 300μm-core-diameter-PS wire with a liquid sample in the cladding region. The dispersion dips between water and alcohol liquids also have a 58%-variation, which corresponds to the theoretical prediction in Fig. 3(a). However, there is a discrepancy in terms of the wavelength position of the waveguide dispersion dips between theory and the measured result shown in Fig. 3(a) and (b), which is more obviously for sensing of water. It could possibly be resulted from the high index of water which is larger than the PS core index to make the dip shift to long wavelength range [25]. Nevertheless, it did not affect qualitative understanding and calculation of dip-variation of waveguide dispersion induced from different cladding index. Notably, the material dispersion of water and alcohol did not be taken into account in the calculated waveguide dispersion shown in Fig. 3(a). For example, the calculated material dispersion of water [26] is on the order of 10^{-6} ps/Km/nm at wavelength range of 0.8~1.1 mm although the refractive index of water is obviously changed from 2.5 to 2.8 at this range [23]. Therefore, the material dispersion of water is small enough compared with the measured waveguide dispersion of PS wire with a water cladding (~-20 ps/Km/nm at dip shown in Fig. 3(b)) and the neglect is reasonable. Based on the variation of waveguide dispersion ΔD_{WG}, different samples can be easily distinguished, such as the water and alcohol in the experiment. According to Fig. 1(b), waveguide dispersion variations ΔD_{WG} of several percent can be detected when the effective

#117682 - $15.00 USD Received 24 Sep 2009; revised 23 Oct 2009; accepted 23 Oct 2009; published 27 Oct 2009
(C) 2009 OSA

cladding index is increased by 0.02. This finding suggests that the THz plastic wire based evanescent sensor enables one to distinguish the slight variation of specimen concentration in solutions, corresponding to cladding index variation, based on the variation of the waveguide dispersion dip.

According to our results, a small amount of plastic powders, polyethylene (PE) (434272 ultra-high molecular weight, surface-modified polyethylene powder, Sigma-Aldrich Inc.) and melamine (Melamine, Nippon Bacterial Test Co., Ltd.), with the grain size of several tens micrometers are mixed in alcohol solutions separately with various concentrations. In general, the pure PE cannot be dissolved in alcohol; however, the PE powders with high molecular weight and a modified polar surface would be slightly dissolved in polar liquids [27]. In the alcohol solution, melamine powders are slightly solute [28] and its solubility [29] could be larger than PE powders due to the polar molecular structure. We stirred the melamine (PE) alcohol solution in a beaker uniformly for several minutes. When turn off the stirrer, we instantly transferred the solution into the PP sample holder by a micropipette before the un-dissolved powders settled to the bottom of the beaker.

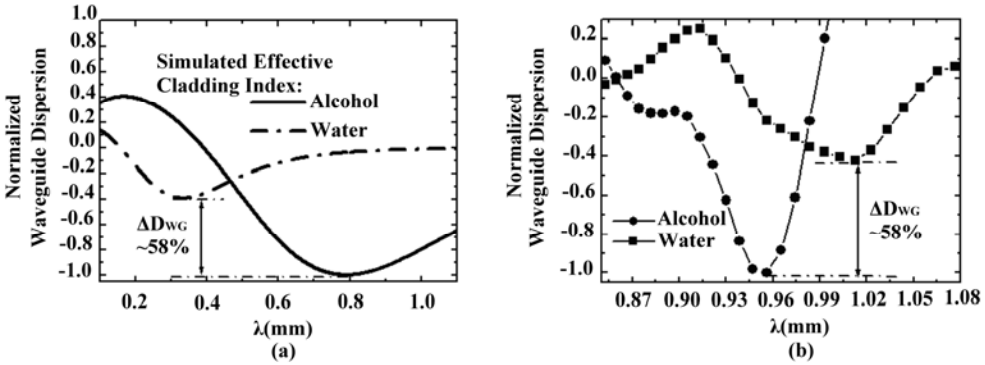

Fig. 3. (a) Simulated waveguide dispersion of 300μm-core-diameter-PS wire with an alcohol-cladding and a water-cladding. Notably, ΔD_{WG} in the graph represents the decreased percentage of waveguide dispersion dips. (b) The measured waveguide dispersions for 300μm-core-diameter-PS wire with liquid claddings of water and alcohol.

The prepared melamine and PE alcohol solutions are with different concentrations, 20~100ppm (part per million, i.e. one milligram-powder per one liter of alcohol in this case), and the waveguide dispersion of THz pulse was measured by THz-TDS system. Figures 4 (a) and (b) display the measured waveguide dispersions of THz pulse traveling on the 300μm-core-diameter-PS wire with melamine and PE alcohol solutions in the cladding region and the concentrations range from 0ppm to 100ppm. Notably, variations of waveguide dispersion dips are observed in Fig. 4(a) while increasing the melamine concentration from 20ppm to 80ppm in alcohol solutions. However, the apparent deviation of waveguide dispersion dips from the PE-alcohol solution observed only when the PE concentration is altered from 20ppm to 40ppm. Because the effective cladding index of PS wire is changed with the solute concentration in alcohol, the waveguide dispersion of THz evanescent wave is modified and correlates with the theoretical prediction shown in Fig. 1(b). In Figs. 4(a), the percentage of variation of waveguide dispersion in relation to pure alcohol, ΔD_{WG}, is approximately proportional to the increased concentration of melamine powder in the alcohol solution. Additionally, the rising of the waveguide dispersion dips apparently ceases even when more powders are mixed in the alcohol due to the saturation of alcohol, i.e. 80ppm and 40ppm for melamine and PE powders, respectively. At the saturation excess situation, the un-dissolved powders will be suspended in the solution. However, the material dispersion of the suspended grains in the alcohol solution could be neglected, compared with the measured waveguide dispersion (with the dip value ranged from –40 to –60 ps/Km/nm in Fig. 4(a)), because the analysis of material dispersion in THz-TDS for PE and melamine bulks reveals that the

#117682 - $15.00 USD Received 24 Sep 2009; revised 23 Oct 2009; accepted 23 Oct 2009; published 27 Oct 2009
(C) 2009 OSA

intrinsic dispersions (~10^{-4} ps/Km/nm) are negligible, as shown in Fig. 4(c). Additionally, the extremely small amount of the suspended grains (~several tens ppm in this experiment) in the alcohol solution are difficult to modify the overall index of alcohol solution. This is because the n_{sample} in Eq. (5) could be approximated to $(1-\rho).n_{solution}+\rho.n_{grain}$ where ρ denotes the concentration of suspended grain on the order of 10^{-6}, and thus the effective cladding index is almost the same as the saturation case. In the saturation excess condition, the waveguide dispersion induced by the suspended powders is so small that it almost cannot affect the measured waveguide dispersion curve from the dissolved solute. For example, when PE powder concentration exceeds 40ppm, as shown in Fig. 4(b), the waveguide dispersion curve does not change, indicating no matter the material dispersion or waveguide dispersion contributed from the suspended grains in the alcohol solution could not affect the measured waveguide dispersion. Therefore, the deviation of the measured waveguide dispersion is attributed to the dissolved materials in the alcohol solution.

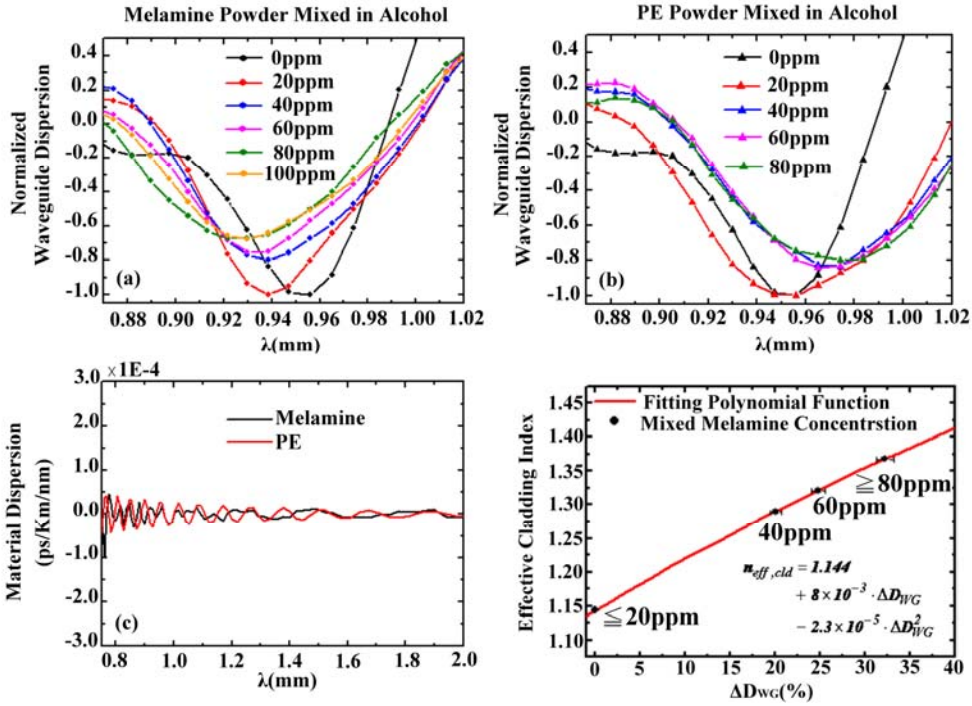

Fig. 4. (a) Normalized waveguide dispersions for various mixed melamine concentrations in alcohol. (b) Normalized waveguide dispersions for various mixed PE powder concentrations in alcohol. (c) Material dispersion of melamine and PE bulk materials. (d) Linear relation of effective cladding index and the dip-variation of waveguide dispersion derived from the melamine powder mixed in an alcohol solution at concentration of 20ppm to 80ppm. The effective cladding indices for different concentrations are referred to the waveguide dispersion dips located in the wavelength range of 0.93~0.94mm.

Closely examining Figs. 4(a) and (b) reveals that the same mixed powder concentrations, 40ppm, of melamine and PE induce 21%- and 18%- ΔD_{WG}, respectively. This finding suggests that an alcohol solution can dissolve more melamine powder than the PE powder. Such an observation is reasonable since the polar molecular structure of melamine has a higher dissolution in the polar liquid, alcohol, compared with the non-polar molecular structure of PE powder. Figure 4(d) shows the linear relation between the measured ΔD_{WG} and effective cladding index for the melamine alcohol solution, in which the solid line denotes the linear fit by polynomial. The +/−1% error bars of the measured ΔD_{WG} at wavelength range of 0.93~0.94mm are also added in Fig. 4(d), which is induced from the measurement variations

#117682 - $15.00 USD Received 24 Sep 2009; revised 23 Oct 2009; accepted 23 Oct 2009; published 27 Oct 2009
(C) 2009 OSA

of phase difference in THz-TDS system. Based on the polynomial equation in Fig. 4(d), the effective cladding index can be estimated from any known measured ΔD_{WG}. The polynomial equation is accurate to the second terms corresponding to two decimal places of effective cladding index. THz refractive indices of the samples can thus be calculated from Eq. (5). For example, 58%-ΔD_{WG} of pure water observed in Fig. 3(b) is applied in the fitting curve and the calculated refractive index of water is 2.66, which is around 2%-deviation compared with the standard water index of 2.60 [22] at 0.9mm-wavelength. Incorporation of +/−1% deviation of ΔD_{WG} in water index calculation, the calculated refractive index of water is ranged from 2.65 to 2.67. It indicates that the deviation of the calculated specimen index, which is induced from the error (+/−1%) in the measured waveguide dispersion, is within 3% compared with its standard. For the sensing results of melamine alcohol solution, the effective cladding index of alcohol is increased with the solute concentration from 1.144 to 1.290 (40ppm), 1.322 (60ppm) and 1.368 (80ppm). Moreover, according to Eq. (5), the respective indices of melamine alcohol solution can be derived as 1.91, 2.00 and 2.15, which are all larger than the original index of pure alcohol, 1.45. This finding suggests that evanescent wave sensing based on subwavelength THz plastic wire provides adequately high sensitivity and reliability to identify minute index variation and the sensitivity can reach the order of 0.01.

5. Conclusions

A noninvasive and label-free THz evanescent wave sensing based on subwavelength plastic wire has been demonstrated for liquid detection. The enhanced evanescent wave causes considerable variation of waveguide dispersion when the cladding index change. Additionally, the dispersion deviation of guided THz wave is measured and two liquids with transparent appearances, water and alcohol, are easily distinguished, which is consistent with theoretical predictions. Based on the measured variation of waveguide dispersion dip, various concentrations of melamine alcohol solution are successfully identified. Moreover, the detection limit is on the order of 20ppm, corresponding to 0.01 index variation in cladding. The THz subwavelength plastic wire based evanescent wave sensor is highly promising for use in various minute material detections, such as illicit drugs or explosives, as well as molecular dynamic detection such as to monitor the product generation rate in the chemical or physical reaction.

Acknowledgment

This work was supported by the Advanced Optoelectronic Technology Center, National Cheng Kung University, under projects from the Ministry of Education and the National Science Council (NSC 97-2218-E-006-013 and NSC 98-2221-E-006-014-MY2) of Taiwan. The authors are grateful for the preparation of plastic wires by the researcher, J.L Kuo, in department of nanofiber materials, Industrial Technology Research Institute.

#117682 - $15.00 USD Received 24 Sep 2009; revised 23 Oct 2009; accepted 23 Oct 2009; published 27 Oct 2009
(C) 2009 OSA